DOI: 10.3901/CJME.2015.0922.113, available online at www.springerlink.com; www.cjmenet.com

3D Two-way Coupled TEHD Analysis on the Lubricating Characteristics of Thrust Bearings in Pump-turbine Units by Combining CFD and FEA

ZHAI Liming[1, 2], LUO Yongyao[1, 2], WANG Zhengwei[1, 2, *], and LIU Xin[1, 2]

1 *State Key Laboratory of Hydroscience and Engineering, Tsinghua University, Beijing 100084, China*
2 *Department of Thermal Engineering, Tsinghua University, Beijing 100084, China*

Received November 7, 2014; revised May 7, 2015; accepted September 22, 2015

Abstract: The thermal elastic hydro dynamic (TEHD) lubrication analysis for the thrust bearing is usually conducted by combining Reynolds equation with finite element analysis (FEA). But it is still a problem to conduct the computation by combining computational fluid dynamics (CFD) and FEA which can simulate the TEHD more accurately. In this paper, by using both direct and separate coupled solutions together, steady TEHD lubrication considering the viscosity-temperature effect for a bidirectional thrust bearing in a pump-turbine unit is simulated combining a 3D CFD model for the oil film with a 3D FEA model for the pad and mirror plate. Cyclic symmetry condition is used in the oil film flow as more reasonable boundary conditions which avoids the oil temperature assumption at the leading and trailing edge. Deformations of the pad and mirror plate are predicted and discussed as well as the distributions of oil film thickness, pressure, temperature. The predicted temperature shows good agreement with measurements, while the pressure shows a reasonable distribution comparing with previous studies. Further analysis of the three-coupled-field reveals the reason of the high pressure and high temperature generated in the film. Finally, the influence of rotational speed of the mirror plate on the lubrication characteristics is illustrated which shows the thrust load should be balanced against the oil film temperature and pressure in optimized designs. This research proposes a thrust bearing computation method by combining CFD and FEA which can do the TEHD analysis more accurately.

Keywords: pump-turbine, thrust bearing, TEHD lubrication, two-way coupled, CFD, FEA

1 Introduction

Large hydrodynamic thrust bearings are the bearings which, due to hydrodynamic lubrication, allow large axial load to be transferred from a moving part (shaft) to the stationary part via a thin layer of the lubricant, thus providing extremely low friction and practically no wear[1]. Thrust bearings are one type of sliding bearing that act as a key component in hydroelectric generating units. The thrust bearing carries both the entire weight of the rotating parts in the unit and the axial hydraulic thrust in the turbine, so it plays an important role in the operating stability. The thrust bearing includes a thrust collar, a mirror plate and several pads. The rotor load is transferred to each pad through the thrust collar and the mirror plate, and then to the base. Every narrow clearance between the mirror plate and each pad is filled with the lubricating oil during operation. The strong fluid-solid interactions among the pads, oil and mirror plate greatly affect the bearing characteristics. The oil film is heated by viscous friction, but the temperature distribution in the angular direction is not uniform, and results in elastic and thermal deformation in the pads and mirror plate which changes the film shape and affects the lubrication characteristics. The elastic deformation of the pad that compensates for the thermal deformation was described by ETTLES, et al[2] in 1963 and was further discussed by DĄBROWSKI, et al[3] (Fig. 1). The bearing pad tends to form a convex shape because of the temperature gradient through its thickness, while the hydrodynamic pressure tends to make the pad concave. The resulting total deflection of the pad then turns out to be fairly small. The thermal deformation is mostly determined by the temperature difference between the top and bottom of the pad, and seldom by the thickness of pad. The elastic deformation is strongly affected by the pad thickness, support dimension, and oil film pressure.

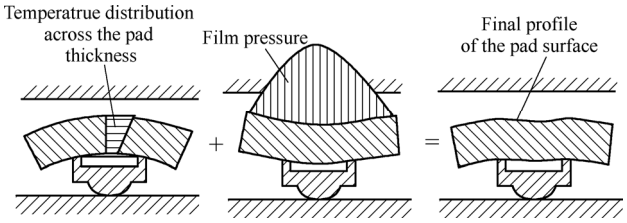

Fig. 1. Schematic diagram of TEHD effects in thrust bearing[3]

* Corresponding author. E-mail: wzw@tsinghua.edu.cn

Supported by National Natural Science Foundation of China (Grant No. 51439002), Specialized Research Fund for the Doctoral Program of Higher Education of China (Grant Nos. 20120002110011, 20130002110072), and Special Funds for Marine Renewable Energy Projects (Grant no. GHME2012GC02)

In conventional hydroelectric generating units, the thrust bearing provides unidirectional rotation with an offset between the supporting center and the pad center. Its circumferential eccentricity of 0.58–0.60 gives the best thrust load capacity[4]. However, pump-turbine units both generate electricity and pump water. Thus, the thrust bearing rotates in both directions and needs good lubrication in both the forward and backward directions. Therefore, the bearing is typically designed as a concentric structure with a circumferential eccentricity of 0.5. The problem is that the support center of the bidirectional thrust bearing is offset from the best location which is not able to form the best wedge shaped film. Consequently, the load capacity of the bidirectional thrust bearing is much lower with poor overall performance. Therefore, the key problem in bidirectional thrust bearing designs is to ensure that the design provides sufficient load capacity.

Accurately predicting the performance of thrust bearings in large hydroelectric generating units, particularly the minimum thickness, the maximum pressure and the maximum temperature in the oil film, is the key to the bearing design. Therefore, analysis with combining the oil film, collar and pads are needed to design a good thrust bearing. At present, there are three main methods used to analyze the lubricating performance of thrust bearings: the hydro dynamics method (HD), the thermal hydro dynamics method (THD), and the thermal elastic hydro dynamics method (TEHD).

The hydrodynamics method solves the generalized Reynolds equation to get the pressure characteristics of the oil film. CHRISTOPHERSON[5] and COPE[6] developed the HD model for thrust bearings and discussed the basic lubrication characteristics of bearing. However, the generalized Reynolds equation was derived by simplifying the Navier-Stokes equations and neglecting the inertia. CHEN, et al[7], presented a 3D CFD model for a sliding bearing and compared the computational results with results using the Reynolds equation to show that the CFD method was more accurate.YU, et al[8], did a HD simulation of gap flow of sector recess multi-pad hydrostatic thrust pad with CFD method. The CFD model in this computation only includes the flow field between the pad and runner. The results show a great influence of recess area on the bearing performance. Similarly HAN, et al[9], computed the hydrodynamic lubrication of microdimple textured surface using 3D CFD. WANG, et al[10], built a 3D CFD model for the thrust bearing in Three-Gorge hydropower station. Not only the oil film but also the flow around the pad in the oil tank were modeled. The oil is considered as an incompressible isothermal Newtonian fluid. The effects of the oil film clearance size and rotational speed on the load capacity were discussed.

The thermal hydrodynamics method for thrust bearings simultaneously solves the generalized Reynolds equation and the energy equation to obtain the temperature distribution in the film. This method was promoted by DOWSON, et al[11–12] who also took into account the temperature-viscosity variation in the oil, but excluded the conjugate heat transfer between the oil film and the pad. LIU[13] analyzed the thrust bearing in a hydro turbine unit in a similar way not consideration the heat transfer in the pad. Further research considered the heat transfers of the pad and mirror plate. GERO, et al[14], used a 3D thermal-fluid FEM model to compute the conjugate heat transfer between the oil film and the pad working surface. The improvements seen in thermal hydrodynamics studies and in experimental results have been discussed in several reviews[15–18]. The coupling of the Reynolds and energy equations increases the computational difficulties for those problems. YU, et al[19], included the thermal effect on the analysis of a thrust washer. The results demonstrated that the thermal effect not only decreased the load and friction, but also increased the side leakage. The effect becomes more obvious with increasing depth of the oil groove. DADOUCHE, et al[20], experimented and analyzed the heating effects in a hydrodynamic thrust bearing with a fixed geometry and compared the experimental results with thermal hydrodynamics model results from numerical simulations, showing that the agreement was satisfactory, but the differences were observed because the elastic deformations of the pad and collar in model were neglected. Recently, WASILCZUK, et al[21–23], also conducted some THD computation with CFD software.

The mechanical deformations of the pad and mirror plate significantly change the oil film shape and greatly affect its lubrication. However, the thermal hydrodynamics model does not fully account for the elastic and thermal deformation of the pad and the mirror plate which has been the main shortcoming of thrust bearing designs for large hydroelectric generating units. In recent years, the computation accuracy has been improved by using thermal elastic hydrodynamics method. STEMLICHT, et al[24], used an adiabatic TEHD model of the pad deformation that considered the pressure and temperature gradients. 3D models of lubrication characteristics of thrust bearings have included Babbitt and PTFE (Polytetrafluoroethylene) layers[25–28]. ZHAO, et al[29], did TEHD analysis for the thrust bearing and demonstrated that the working behavior of the thrust bearing with pivoted supports is better than that of the bearing with single-point supports. AHMED, et al[30], analyzed a thrust bearing using the thermal elastic hydrodynamics method and compared their results with the numerical and experimental results in the previous study[20]. The comparison shows that the accuracy is improved by considering both the thermal and elastic deformation in the pad and mirror plate. JIANG[31] also employed a TEHD model to analyze the effects of deformation, rotational speed, load and oil viscosity grade on lubrication performance of a tilting pad thrust bearing of a hydro turbine. BORRÀS, et al[32], built a multiphysics (TEHD) model of spring-supported thrust bearings for hydropower applications. KARADERE[33] investigated the effects of the total bearing deformation on the

performance of hydrodynamic thrust bearings. Recently, a lubrication analysis program has been combined with ANSYS in a thermal elastic hydrodynamics of a thrust bearing with good agreement with measured results[34–36]. More studies about TEHD lubrication can be found in some dissertations[37–41].

The main thermal elastic hydrodynamics method seen in the literatures above to analyze the lubrication of thrust bearings combines the Reynolds equation and FEA: (1) solving the generalized Reynolds equation to get the oil film characteristics using the finite difference method, (2) analyzing the structure characteristics using a FEA model, and (3) exchanging the temperatures, pressures, and displacements in (1) and (2) to complete the thermal elastic hydrodynamics analysis. However, the generalized Reynolds equation was derived from the Navier-Stokes equations by neglecting the inertia and film curvature. In this method, the oil tank inlet temperature or measured temperature are set as the temperature boundary condition of the film, but the condition differs from real situation. In addition, the finite difference method is not suitable for solving the Reynolds equation when there are complex sliding bearing surfaces. It is easy to combine CFD and FEA in THD analysis by solving liquid-solid conjugate heat transfer equations or in EHD analysis, but difficult to solve the TEHD analysis. Till now, most researches of thrust bearings combine Reynolds equation and FEA to solve the TEHD problem. However, little literature has been found on the TEHD lubrication computation for the thrust bearing combing CFD and FEA.

Aimed to develop TEHD solution method, this paper will conduct a fluid-solid-thermal two-way coupled solution for a bidirectional thrust bearing in which a 3D computational fluid dynamics model (CFD) for the oil film and a 3D finite element analysis model (FEA) for the pads are combined. Considering the viscosity variation with the temperature, the three-field model coupling the thermal, structural and fluid effects combing CFD and FEA is developed successfully. More reasonable boundary conditions can then be set for the oil film and the bearing lubrication characteristics can be more accurately analyzed. Furthermore, the effects of rotational speed on the lubrication performance are also discussed.

2 Two-way Coupled Computational Theory for the Thermal Elastic Hydro Dynamics Model Combining CFD and FEA

The lubrication of a large thrust bearing is a very complex process with varying temperature and pressure in the oil film as well as thermal and elastic deformation in the pads and the mirror plate. The pressure, temperature and thickness of the oil film between the pad and mirror plate can be used as performance indexes for the thrust bearings. The three important parameters are determined by various factors such as the load, rotational speed, oil inlet temperature, oil viscosity, pad dimensions and geometry, pad deformation, material properties, mirror plate planeness, and so on. The different materials used for the pad and mirror have different elastic modulus, thermal resistances and thermal expansion coefficients which greatly influences the lubrication characteristics. The equations for momentum, energy, viscosity-temperature variation, heat conduction, deformation should be solved simultaneously by iteration to obtain the pressure and viscosity variations, and the thermal elastic deformations to accurately describe the lubrication characteristics.

2.1 Fluid control equations

The Navier-Stokes equations were solved for the oil film flow considering the effect of the inertia force and body force terms. The computational fluid dynamics method was used to solve the momentum, continuity and energy conservation equations for laminar, three-dimensional flow. The lubricant was treated as a single-phase incompressible Newtonian fluid. Here, steady process is assumed.

The momentum equation is

$$\frac{\partial \rho_f v}{\partial t} + \nabla \cdot (\rho_f v v - \tau_f) = f_f. \tag{1}$$

The continuity equation is

$$\frac{\partial \rho_f}{\partial t} + \nabla \cdot (\rho_f v) = 0. \tag{2}$$

Where t is the time, ρ_f is the fluid density, f_f is the body force vector in the fluid, v is the fluid velocity vector and τ_f is the shear stress tensor,

$$\tau_f = (-p + \mu \nabla \cdot v) I + 2\mu e, \tag{3}$$

where p is the fluid pressure, μ is the fluid dynamic viscosity and e is the stress tensor, and

$$e = \frac{1}{2}(\nabla v + \nabla v^{\mathrm{T}}).$$

The energy conservation equation is

$$\frac{\partial (\rho h_{tot})}{\partial t} - \frac{\partial p}{\partial t} + \nabla \cdot (\rho_f v h_{tot}) = \nabla \cdot (\lambda \nabla T) + \nabla \cdot (v \cdot \tau) + v \cdot \rho f_f + S_E, \tag{4}$$

where λ is the fluid thermal conductivity and S_E is the energy source term.

The dynamic viscosity of the lubricating oil decreases as oil temperature increases, especially significantly at low oil temperatures. Generally the relationship between the viscosity and the temperature is expressed as an

exponential function as follows:

$$\mu(T) = \mu_s \exp(-\beta(T - T_s)), \tag{5}$$

where μ_s is the dynamic viscosity of the oil at T_s; T is the absolute temperature, T_s is the oil temperature at the oil tank inlet, and β is the viscosity-temperature coefficient, which is obtained using two dynamic viscosities at two different temperatures.

As the lubrication oil is incompressible, the density-temperature and density-pressure effects are ignored in this study.

2.2 Solid control equations

The solid motion conservation equation derived from Newton's second law is

$$\rho_s \ddot{d}_s = \nabla \cdot \sigma_s + f_s, \tag{6}$$

where ρ_s is the solid density, σ_s is the Cauchy stress tensor, f_s is the body force vector in the solid and $\ddot{d}_s$ is the local acceleration vector of the solid domain.

The thermal deformation term induced by the temperature difference is

$$f_T = \alpha_T \cdot \nabla T, \tag{7}$$

where α_T is the thermal expansion coefficient.

The thermal boundary conditions at the pad are as follows.

The working surface of the pad is

$$T_{pad} = T_{oil}, \left(k\frac{\partial T}{\partial z}\right)_{pad} = \left(k\frac{\partial T}{\partial z}\right)_{oil}. \tag{8}$$

The other surface of the pad is

$$-\left(k\frac{\partial T}{\partial n}\right)_{pad} = \alpha_i (T - T_\infty), \quad i=2,\ 3,\cdots, \tag{9}$$

where T is the wall temperature, T_∞ is the oil tank temperature; and α_i is the empirical convective heat transfer coefficient to the pad surface.

The convective heat transfer coefficient on the pad bottom surface was given by Ettles[17]

$$\alpha_i = 92.3 N^{0.7} r^{0.3} \mu^{-0.2} \theta^{-0.4}. \tag{10}$$

The convective heat transfer coefficient on the mirror plate and the thrust collar were based on the rotating disk Shilts' number

$$\alpha_i = 480\sqrt{N}\mu^{-0.05}. \tag{11}$$

2.3 Thermal elastic hydro dynamic interaction (FSI) equation

In fact, two methods can be used to solve fluid-structure interaction problems, the direct coupled solution and the separate coupled solution. The equations governing the flow and the structural displacement were solved simultaneously with a single solver as a directly coupled method, which is better for FSI problem since it is faster and more stable. This method has been used to deal with many magnetic-structure, thermal-structure, and simple fluid-structure problems. The separately coupled solution method sequentially solves separate fluid and solid control equations in a single solver or different solver with the results exchanged at the fluid-solid interface without conservation of the energy at the interface. The separately coupled solution method can make full use of the existing computational fluid dynamics and computational solid mechanics methods with a low memory usage. Eq. (12) describe the data exchanging method in thermal elastic hydro dynamic interaction which requires conservation of pressure, displacement, thermal flux, and temperature at the interaction interface:

$$\begin{cases} \tau_f \cdot n_f = \tau_s \cdot n_s, \\ d_f = d_s, \\ q_f = q_s, \\ T_f = T_s, \end{cases} \tag{12}$$

where the subscript f denotes fluid and s denotes solid.

In this study, the TEHD analysis on the thrust bearing is conducted using the direct coupled method for the fluid-thermal field in the oil film and for the solid-thermal field in the pad and mirror plate respectively, and using the separately coupled for the data exchanging between oil film and the pads (or the mirror plate) as shown in Fig. 2. Specifically, the fluid thermal field in the oil film was first calculated by solving the energy equation and Navier-Stokes equations with the viscosity-temperature relationship in the oil film. Then the pressure and temperature on the interface between the oil film and the pad (or the mirror plate) were transferred to the pad (or the mirror plate). Next, the solid thermal fields in the pad and mirror plate were computed with the directly coupled solution method again. Last the deformation and temperature on the interfaces were transferred to the oil film to act as the boundary condition in the oil film computation in the next iteration. Thus the loop iteration was executed to achieve the convergence. In this study, the global convergence target is 0.01 for displacement, force and temperature on the interface. In short, the direct coupled method was used to calculate the fluid thermal field in the oil film and the thermal-structure filed in the pad (or the mirror plate), while the separately coupled method was used for the coupling between the oil film and the pad (or the mirror plate).

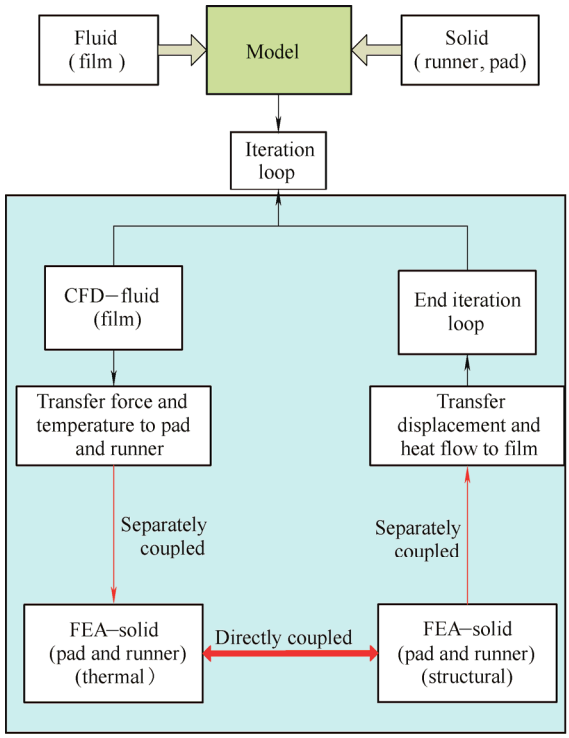

Fig. 2. Iteration process for the TEHD lubrication two-way coupled solution

3 Numerical Computation Model

The thrust bearing includes the thrust collar, mirror plate, pad, and bearing seat as shown in Figs. 3(a), 3(b), 3(c). The thrust collar is fixed to the rotor shaft by bolts and rotates with the rotor shaft. The mirror plate is installed below and fixed to the thrust collar. The thrust bearing is installed in a closed lubricating oil tank. Ten sector pads are supported by the elastic oil tanks that are self-adjusting connected to pressurized oil pipes with each other. The forces acting on the pads are balanced by the sides of the elastic oil tank. The oil tanks support the pads with a circumferential eccentricity of 0.5. The location of temperature measurement point is arranged in the center of the layer 20 mm below the pad sliding surface as shown in Fig. 3(d).

In this study, it is assumed that the load is equally shared by all bearing pads (no misalignment). This assumption allows for considering only one pad with cycle symmetry condition in the computation model. So this simulation used 1/10 of the model because there are 10 pads evenly arranged along the circumference. The bearing is treated to be fully flooded in the oil, and its pad material to be homogenous and isotropic with on coating on the sliding surface. The hydrostatic recess on the pad to support the unit weight during startups and shutdowns was also omitted, so did the inlet and outlet chamfers to simplify the model, because this paper focus on the achieving the combination of CFD and FEA in the TEHD analysis. The structural parameters are listed in the Table 1. A dynamic mesh is used to model the oil flow field. After grid independent check, 8140 elements for the film and 14 426 elements for the structures are selected. There are respectively 40 and 50 layer meshes in the radial and angular direction, as well as 10 layer meshes in the axial direction in the oil film. The interfaces between the pad and the oil film, and between the mirror plate and the oil film are fluid-solid-thermal coupling interfaces. The boundary conditions are shown in Fig. 4 with the operation condition listed in Table 2. The convective heat transfer coefficients of pad free surfaces were decided according to HUANG's study[42]. Contact elements were used for the interaction between the pad and the oil tank.

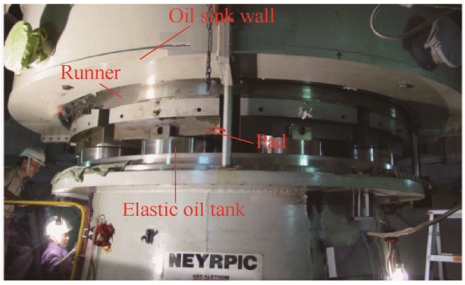

(a) Main components

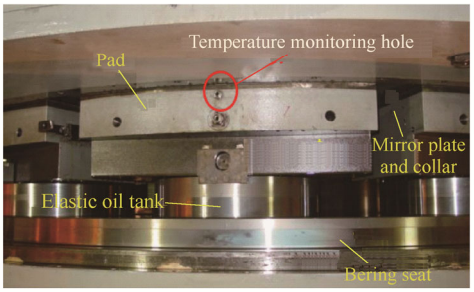

(b) Main components

(c) Pad

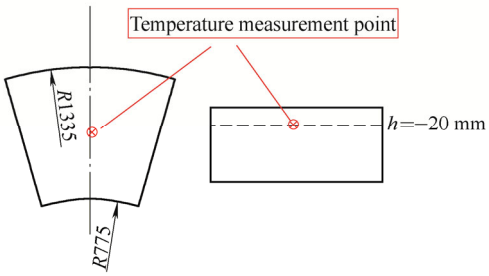

(d) Location of the temperature measurement point

Fig. 3. Structure of the thrust bearing

Table 1. Thrust bearing structural parameters

Item	Value
Outer radius of pad R_1/mm	1335
Inner radius of pad R_2/mm	775
Pad angle θ/(°)	31
Outer radius of thrust collar R_3/mm	1335
Inner radius of thrust collar R_4/mm	775
Pad thickness H_1/mm	203
Number of pads n	10
Total thrust load F/t	200
Collar thickness H_2/mm	660
Rotating speed ω/(r • min^{-1})	500
Radial offset of the pad center O_r/mm	0
Circumferential offset of the support center O_c/mm	0

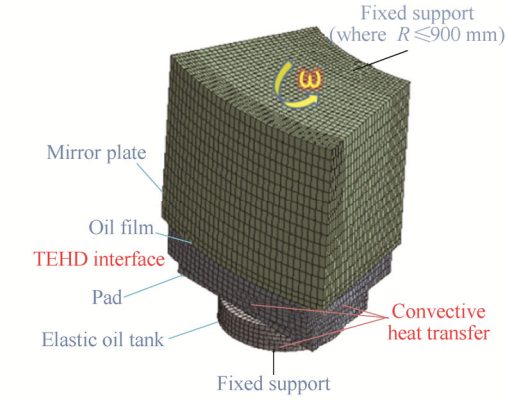

(a) Solid model for the pad and mirror plate

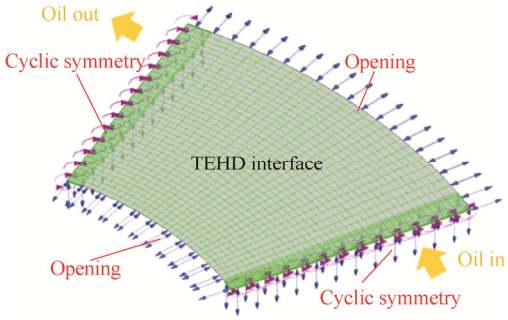

(b) Fluid model for oil film

Fig. 4. TEHD model of the thrust bearing

Table 2. Material properties and operation condition

Item		Value
Ambient oil temperature T/℃		35
Oil density ρ/(kg • m^{-3})		890
Dynamic viscosity of the oil μ_{40}/(Pa • s)		0.036
Dynamic viscosity of the oil μ_{100}/(Pa • s)		0.004 5
Thermal conductivity of oil λ/ (W • m^{-1} • K^{-1})		0.145
Specific heat of oil C/(J • kg^{-1} • K^{-1})		2000
Thermal expansivity of oil α/ K^{-1}		0.000 38
Thermal conductivity of pad λ_p/(W • m^{-1} • K^{-1})		49.8
Specific heat of pad C_p/(J • kg^{-1} • K^{-1})		465
Thermal expansivity of pad α_p/K^{-1}		1.2×10^{-5}
Young's modulus of pad E/Pa		2.12×10^{11}
Poisson's ratio ν		0.27
Convective heat transfer coefficient of pad h_c/(W • m^{-2} • K^{-1})	at the pad bottom	800
	at the leading side	1000
	at the trailing side	1000
	at the inner radius side	1500
	at the outer radius side	2000

The iteration algorithm for the TEHD lubrication two-way coupled solution combining CFD and FEA is illustrated in Fig. 2. It is worth mentioning that initial film thickness, inclined angles along radial and angular direction will be defined in the conventional TEHD method combining Reynolds equation and FEA, while only thickness will be defined in this study. Because the oil flows into the narrow gap and out into oil tank, then leads to high pressure at the inlet and low pressure at the outlet which deforms the pad (or the mirror plate) and forms the inclined angles along radial and angular direction automatically. After one iteration, the computed oil force will be compared with the thrust load. If larger than thrust load, the oil film thickness will increase and recomputed. If lower than the load, the oil film will be thinner and recomputed. This method ensures the force of oil film as the same as the thrust load. Oil film of the thrust bearing is usually very thin in tens of micrometer range which causes the viscous affecting the whole flow field in the film. The Reynolds number is about 127 much less than 1000 based on Eq. (13). So the flow in the oil film is assumed to be laminar.

$$R_e = \frac{\rho \nu L}{\mu}, \tag{13}$$

where ρ is density of the oil film (kg/m^3), ν is line velocity of the outer radius of the mirror plate (m/s), L is the average of the oil film (m), and μ is dynamic viscosity of the oil (Pa • s).

4 Results and Discussions

Converged TEHD results of this case were obtained after 20 interations. The pressure, temperature, oil film thickness distributions, the elastic and thermal deformations of the pad and mirror plate along the circumference and radial directions (Fig. 5) will be discussed herein after.

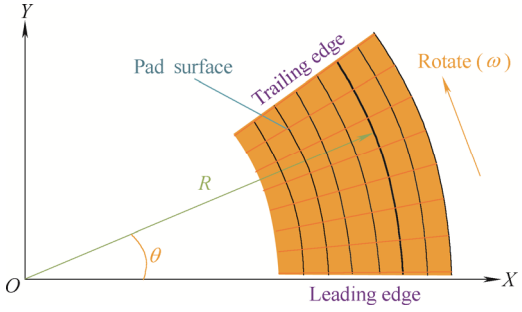

Fig. 5. Schematic diagram of angular and radial directions for the post processing

4.1 Analysis of the film pressure

Unlike the offset support of pads in conventional hydroelectric generating units, the elastic tank of the thrust

bearing for pump turbine units is attached to the bottom center of the pad for bidirectional operation, which makes those two kinds of bearings very different. Fig. 6(a) shows the pressure contour on the pad working surface with the maximum pressure near the center. The mirror plate rotates from the right side (leading edge) to the left side (trailing edge). The pressure distribution agrees well with the measured results for a bidirectional thrust bearing in Ref. [42] shown in Fig. 6(b). By contrast, the maximum pressure usually occurs near the trailing edge on the pad working surface. The pressure along the circumference is shown in Fig. 7(a). The pressure increases first and then decreases from the leading edge towards the trailing edge. At the trailing edge, the pressure drops sharply which may cause cavitation. Fig. 7(b) shows how the pressure varies in the radial direction. The pressure first increases from the inside towards the outside and then decreases. The peak pressure is then at the center and closer to the inside. The predicted thrust force is 201.5 t with a difference 0.75% between the actual thrust force 200 t as shown in Table 3.

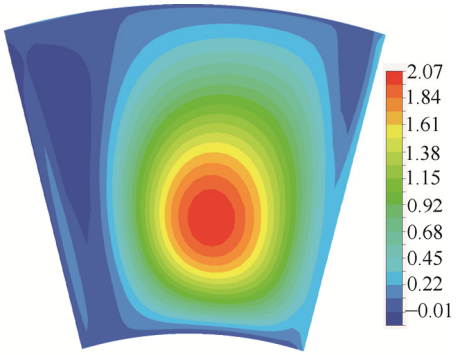

(a) Calculated in this paper

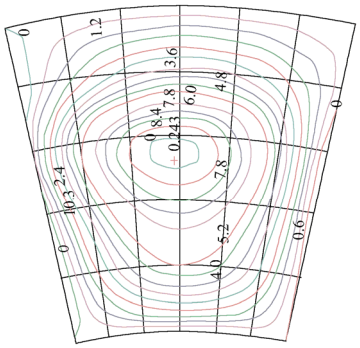

(b) Measured in Ref. [42]

Fig. 6. Pressure distribution on the pad working surface (MPa)

4.2 Temperature characteristics in the oil film

4.2.1 Temperature distribution

When the unit is operated at high rotational speeds, the viscous friction in the oil film produces much heat which results in high temperatures. Thus, the pad and mirror plate are also deformed by the non-uniform temperature gradient. Furthermore, the viscosity as well as the thrust load will be reduced by the increasing temperature.

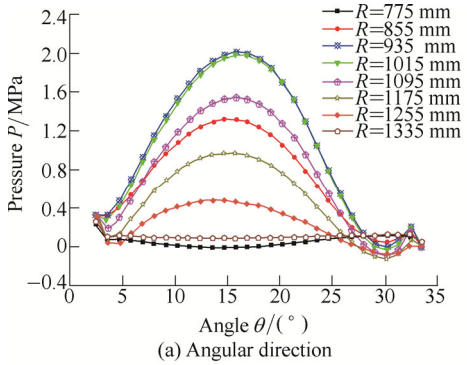

(a) Angular direction

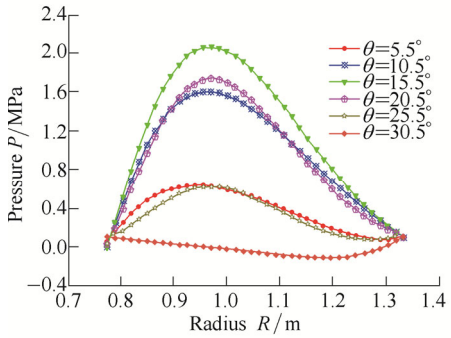

(b) Radial direction

Fig. 7. Pressure distribution on the pad working surface

Table 3. Predicted and measured thrust load

Item	Thrust load F/t	Temperature T/℃
Predicted	201.50	59.85
Measured	200.00	57.00
Deviation ζ/%	0.75	5.00

Fig. 8 shows the temperature distributions on the pad sliding surface both in this present work and Ref. [42]. The temperature distribution tendency on the pad agrees with the measured temperature distribution on the whole as shown in Fig. 8(b). The predicted and measured temperatures are both highest near the trailing edge.

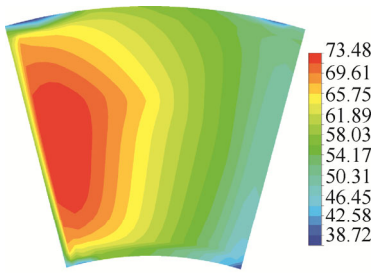

(a) Predicted in the present work

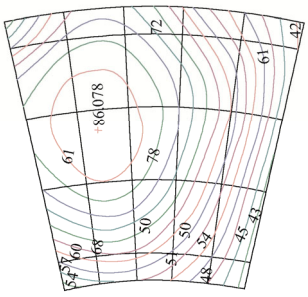

(b) Measured in Ref. [42]

Fig. 8. Temperature distribution on the pad sliding surface (°C)

The temperature increases from the leading edge towards the trailing edge with the maximum of 73.5 ℃ as shown in Fig. 9(a). The film is in a wedge shape with a smaller clearance near the trailing edge, thus, the viscous friction produces more heat near the trailing edge which leads to higher temperatures near the trailing edge. Then, the temperature drops suddenly after reaching the peak because the heated oil flows out of the pad and mixes with the cool oil in the tank. The pad temperature varies gently with slightly higher temperatures at the center which decreases near the outer radius in the radial direction as shown in Fig. 9(b). During the operation, the pad temperature was monitored at the measurement point shown in Fig. 3(d). The measurement point is at the center of the layer 20 mm below the pad working surface. Table 3 shows the predicted temperature is about 5% higher than the measurements. The predicted temperature at this point is about 13 ℃ lower than the maximum on the working surface. Thus, the highest temperature of the working surface can be predicted to be about 70 ℃ from the measuring temperature during operation.

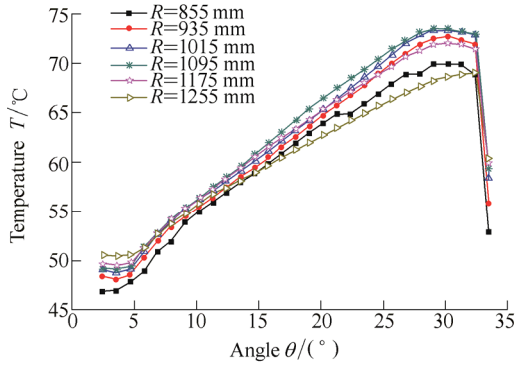

(a) In the angular direction

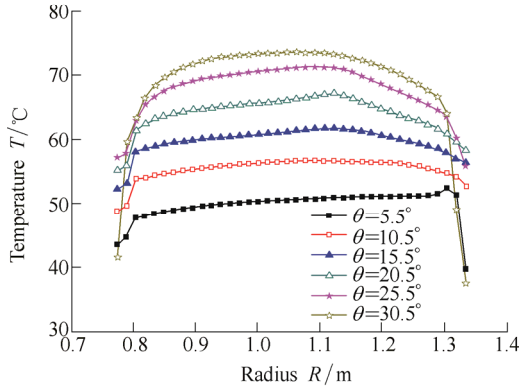

(b) In the radial direction

Fig. 9. Temperature variation on the pad working surface

4.2.2 *Discussion about oil temperature at the leading and trailing edge of the pad*

The cold lubrication oil enters the oil film and removes the friction heat with hot oil leaving the oil film. However, the hot oil is not fully cooled between the adjacent pads and enters the next pad at a higher temperature. Thus, the temperatures at the leading edge and the trailing edge are not equal to that at the oil tank inlet. In the thrust bearing lubrication analysis by solving the generalized Reynolds equation, the temperature boundary condition surrounding the film is usually set as equal to the temperature at the oil tank inlet or as the measured temperature at the film leading edge and trailing edge, which leads to less accurate predicted results. This problem can be solved by using CFD installed of the Reynolds equation. The cyclic symmetric boundary condition was used here for CFD model of the oil film rather than specifying the oil temperatures at the inlet or outlet. The numerical results in Table 4 show that the average temperature at the leading edge is 49.5 ℃ while the trailing edge is 55.4 ℃. Average deviation is the deviation between the average temperature at the leading edge or trailing edge with that at the oil tank inlet. The trailing edge is hotter due to the viscous heating, while the leading edge is cooler because the oil is cooled by the cool oil between two pads before entering the next pad. However, the leading and trailing temperatures are both higher than that at the oil tank inlet (35 ℃) with average deviation of 41.4% and 58.3% respectively, which is close to the actual measurement. Therefore, the rotational symmetric boundary condition for the CFD method used in this study is more reasonable. From this perspective, combining CFD and FEA has this advantage in the TEHD analysis for the thrust bearing.

Table 4. Oil temperature at some key positions

Item	Leading edge	Trailing edge	Tank inlet
Temperature range T/℃	37.4–54.2	34.8–60.6	35
Average value T/℃	49.5	55.4	35
Average deviation ζ/%	41.4	58.3	–

4.3 Deformation of the pad and mirror plate

The oil film is affected significantly by the pad and mirror plate due to the thermal and elastic deformations which can reach the level of the oil film thickness. Fig. 10 shows the deformation on the pad working surface and on the mirror plate surface. The mirror plate rotates from the right side to the left side. The pad tends to form a convex shape due to both the temperature gradient in the pad and the pressure on the pad working surface. The top of the convex surface is near the trailing edge. Fig. 11 shows the axial deformations in angular direction on the pad and mirror plate working surface. The pad surface deformation first increases near the leading edge and then decreases with the peaks close to the trailing edge. The mirror plate deformation is almost constant in the angular direction with only a slight decrease. Thus, the oil film has a wedge shape above each pad in the angular direction due to the deformations, which contributes to form high pressure in the oil film. The deformations distribution along the radial direction on pad and mirror plate is shown in Fig. 12. From the inner diameter to the outer, the mirror plate deformation increases linearly, so the outer edge of mirror plate is lifted

a little as shown in Fig. 12(b).

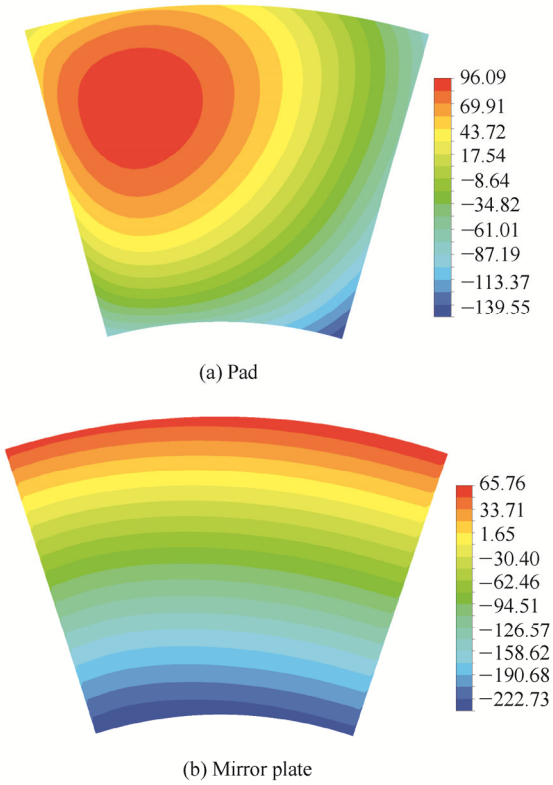

Fig. 10. Deformation distribution on the working surfaces (μm)

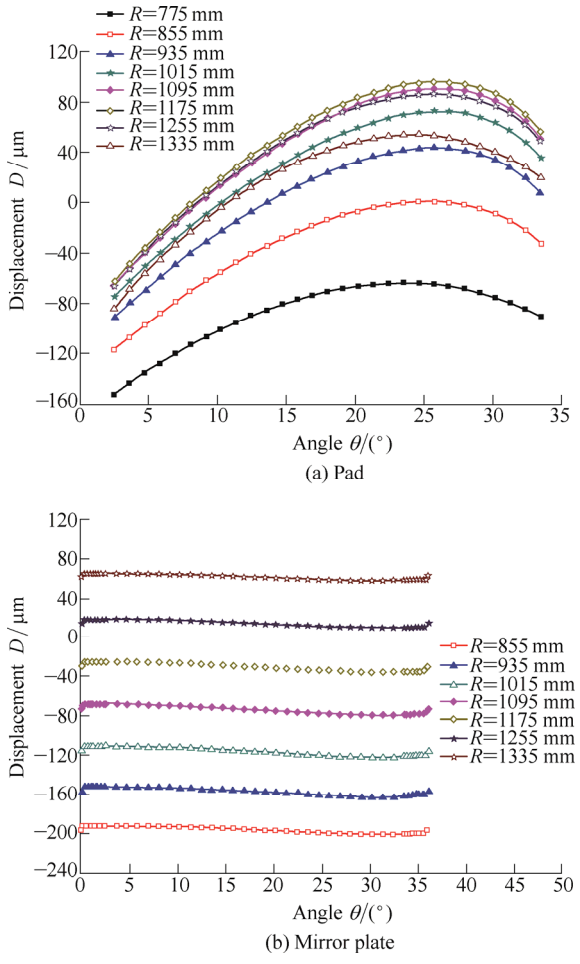

Fig. 11. Axial deformation distribution of the working surface in the angular direction

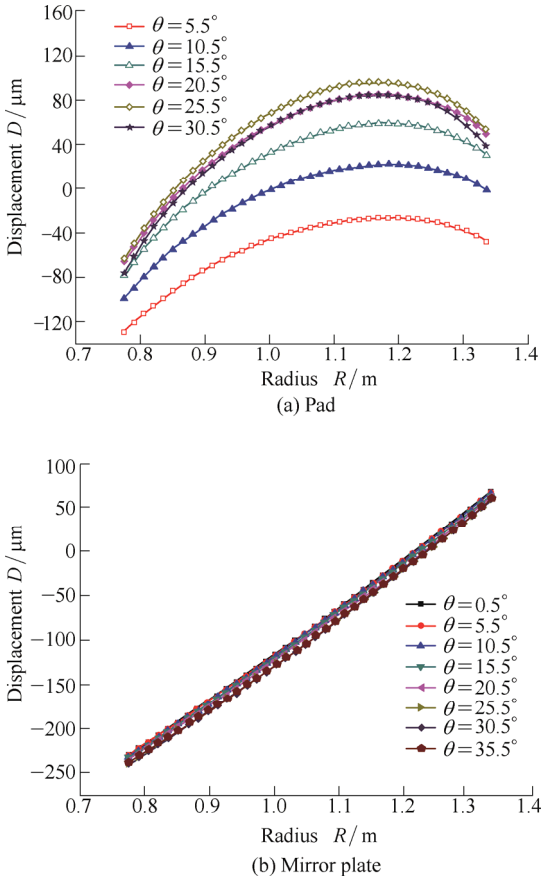

Fig. 12. Axial deformations distribution of the working surface in the radial direction

Because of the thermal and elastic deformation on the pad and mirror plate, the oil film form a wedge shape along the rotational direction with the thickness distribution shown in Fig. 13. The film is thicker relatively at the four corners than the center with a minimum thickness of 28.6 μm near the outlet side.

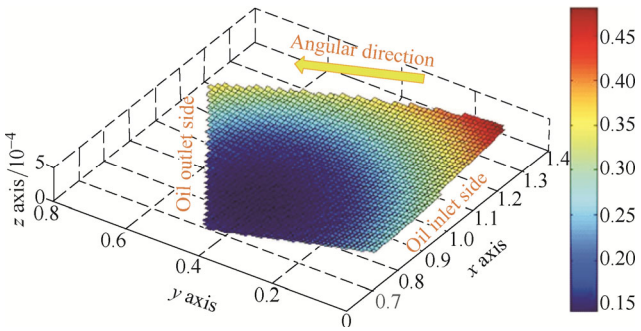

Fig. 13. Oil film thickness distribution (mm)

4.4 Effects of rotational speed on the lubrication performance of the oil film

For the pumped-storage power stations which have been put into production, the rotational speeds of the units are constant during normal operation. So the thrust bearing lubrication calculation for various speeds does not make much of a practical sense. However, during the design stage of the unit, or for the thrust bearing design agency, such studies can help the engineers cognize further about the

characteristics of the thrust bearing and do the optimization. Also pump-turbines units frequently start and stop with great variation in their rotational speed. Here, the TEHD simulation of the thrust bearing were conducted with rotational speeds of 200, 300, 400, 500 and 600 r/min to analyze its effects on the total load and the maximum temperatures and pressures on the pad and the thrust runner surfaces as shown in Fig. 14. The maximum pressure lines of the pad and thrust runner coincide with each other and increase linearly with the rotational speed, so the maximum pressures on the pad and thrust runner are almost the same. The thrust load also increases with the rotational speed. The maximum temperatures on the pad and mirror plate surfaces also increase linearly with the rotational speed, but the pad surface has higher maximum temperatures and greater growth rate. Therefore, increasing the rotational speed can be used to increase the thrust load. However, it is worth noting that too high rotational speed may lead to too high pressure, too high temperature in the oil film, which have negative impact on the performance of the thrust bearing. So the rotational speed should be controlled to ensure the thrust and the oil film temperatures and pressures suitable and achieve an optimal point.

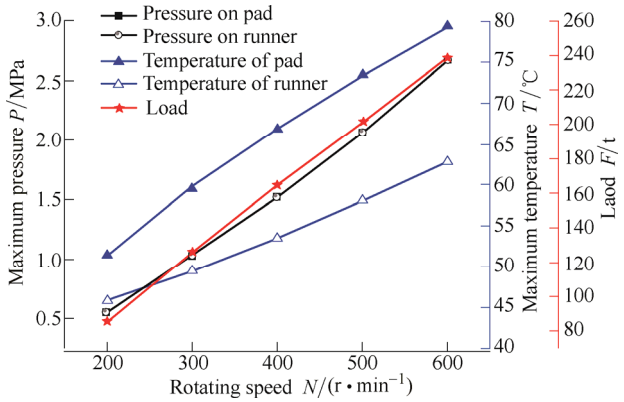

Fig. 14. Effects of rotational speed on the lubrication performance of the oil film

5 Conclusions

In this paper, steady thermal elastic hydro dynamic (TEHD) lubrication considering the viscosity-temperature effect for a bidirectional thrust bearing in a pump-turbine unit was simulated combining a 3D CFD model for the oil film with a 3D FEA model for the pad and mirror plate. The deformations of the pad and mirror plate were predicted and discussed as well as the distributions of oil film thickness, pressure, temperature. Based on the present study, the following conclusions can be drawn.

(1) It has been proved that the TEHD two-way coupled solution for the thrust bearing lubrication with CFD and FEA can be implemented by using both direct and separate coupled solutions together. As more reasonable boundary conditions, cyclic symmetry condition is allowed to use in the oil film flow. Moreover, this method requires no initial inclined angles along radial and angular direction which are necessary in the Reynolds equation solution.

(2) The angular and radial deformations of the pad first increase and then decrease to create a convex working surface. The radial deformation of the mirror plate increases in the radius direction, but changes little in angular direction. As a result, these deformations form a wedge shaped oil film in the angular direction that contributes to increase the pressure.

(3) The average temperature of pad working surface is higher than that of the mirror plate. Measured temperatures inside the pad are lower than the maximum temperature on the pad working surface. The temperatures at the leading edge and trailing edge of the film are higher than the oil temperature at the tank inlet.

(4) As the rotational speed increases, the maximum oil temperature, maximum oil pressure and the thrust all increase. Thus, the thrust should be balanced against the oil film temperature and pressure in optimized designs.

It worth mentioning that there are still some differences in the numerical and the measured results, because the detailed design of the pad and its support is simplified, along with the influence of the hydrostatic pocket. The convective heat transfer coefficients of pad free surfaces are assumed to be constant which is actually not accurate. So future work should be done to improve the numerical method and adopt more appropriate thermal boundaries for the TEHD models, which contribute to obtain more accurate results.

References

[1] WASILCZUK M, WODTKE M, DĄBROWSKI L. Large hydrodynamic thrust bearings and their application in hydrogenerators[J]. *Encyclopedia of Tribology*, 2013: 1912–1926.

[2] ETTLES C M, CAMERON A. Thermal and elastic distortions in thrust bearings[J]. *Inst. of Mech. Engrs., Conf. on Lubr. and Wear*, 1963, 7: 60–71.

[3] DĄBROWSKI L, WASILCZUK M. Evaluation of water turbine hydrodynamic thrust bearing performance on the basis of thermoelastohydrodynamic calculations and operational data[J]. *Proceedings of the Institution of Mechanical Engineers, Part J: Journal of Engineering Tribology*, 2004, 218(5): 413–421.

[4] LUO Z P. Study on centrally supporting thrust bearing[J]. *Dongfang Electric*, 2002, 16: 208–212.

[5] CHRISTOPHERSON D C. A new mathematical model for the solution of film lubrication problems[J]. *Proc. Ins. Mech. Engrs.*, 1942, 146: 126–135.

[6] COPE W F. A hydrodynamic theory of film lubricant[J]. *Proc. Soc. Lond. Ser. A*, 1949, 197: 201–217.

[7] CHEN P Y P, HAHN E J. Use of computational fluid dynamics in hydrodynamic lubrication[J]. *Proceedings of the Institution of Mechanical Engineers, Part J: Journal of Engineering Tribology*, 1998, 212(6): 427–436.

[8] YU Xiaodong, ZHANG Yanqin, SHAO Junpeng, et al. Numerical simulation of gap flow of sector recess multi-pad hydrostatic thrust bearing[C]//*Asia Simulation Conference-7th International Conference on System Simulation and Scientific Computing, IEEE*, 2008: 675–679.

[9] HAN Jing, FANG Liang, SUN Jiapeng, et al. Hydrodynamic

lubrication of microdimple textured surface using three-dimensional CFD[J]. *Tribology Transactions*, 2010, 53(6): 860–870.

[10] WANG Hongjie, GONG Ruzhi, LU Deping, et al. Numerical simulation of the flow in a large-scale thrust bearing[C]//*ASME 2010 3rd Joint US-European Fluids Engineering Summer Meeting collocated with 8th International Conference on Nanochannels, Microchannels, and Minichannels,* American Society of Mechanical Engineers, 2010: 173–180.

[11] DOWSON D, HUDSON J D. Thermohydrodynamic analysis of the infinite slider bearing. Part I: the plane inclinded slider bearing[C]// *Proceedings of the Institute of Mechanical Engineers, Lubrication and Wear Group Convention*, Bournemouth, UK, 1963: 31–41.

[12] DOWSON D, HUDSON J D. Thermohydrodynamic analysis of the infinite slider bearing. Part Ⅱ: theparalled surface bearing[C]// *Proceedings of the Institute of Mechanical Engineers, Lubrication and Wear Group Convention*, Bournemouth, UK, 1963: 42–46.

[13] LIU Fei. *Research on lubricating property of stability condition on large-scale water turbine group*[D]. Wuhan: Huazhong University of Science & Technology, 2008. (in Chinese)

[14] GEROLR, ETTLES C M. A three dimensional thermohydrodynamic finite element scheme for fluid film bearings[J]. *Tribol. Trans.*, 1988, 31(2): 182–191.

[15] KHONSARI M. A review of thermal effects in hydrodynamic bearing. Part 2: Journal bearings[J]. *ASLE Trans.*, 1987, 30(1): 26–34.

[16] FILLON M, FRENE J, BONCOMPAIN R. Historical aspects and present development on thermal effects in hydrodynamic bearings[C]//*Proceedings of the Thirteenth Leeds-Lyon Symposium on Fluid Film Lubrication, Osborne Reynolds Centenary, Elsevier, Tribology Series 12*, 1987: 27–47.

[17] PINKUS O. Anisothermal fluid film in tribology[J]. *J. Tribol.*, 1984, 22: 121–141.

[18] TANAKA M. Recent thermohydrodynamic analysis and designs of thick-film bearings[J]. *Proc. IMechE, Part J: Engineering Tribology*, 2000, 214: 107–121.

[19] YU T H, SADEGHI F. Thermal effects in thrust washer lubrication[J]. *Journal of Tribology*, 2002, 124(1): 166–177.

[20] DADOUCHE A, FILLON M, BLIGOUD J C. Experiments on thermal effects in a hydrodynamic thrust bearing[J]. *Tribol. Int.*, 2000, 33(3): 167–174.

[21] WASILCZUK M, ROTTA G. Modeling lubricant flow between thrust-bearing pads[J]. *Tribology International*, 2008, 41(9): 908–913.

[22] ROTTA G, WASILCZUK M. CFD analysis of the lubricant flow in the supply groove of a hydrodynamic thrust bearing pad[C]// *ASME/STLE 2007 International Joint Tribology Conference, American Society of Mechanical Engineers*, 2007: 307–309.

[23] WASILCZUK M, ROTTA G. On the possibilities of decreasing power loss in large tilting pad thrust bearings[G]. *ISRN Tribology*, 2013.

[24] STEMLICHE B, CARTER G K, ARWAS E B. Adiabatic analysis of elastic, centrally pivoted, sector, thrust-bearing pads[J]. *J. ApplMech.*, 1961, 28: 179–187.

[25] ETTLES C M, ANDERSON H G. Three-dimensional thermoelastic solutions of thrust bearings using code Marmacl[J]. *J. Tribol.*, 1991, 113: 405–412.

[26] DABROWSKI L, WASILCZUK M. Evaluation of water turbine hydrodynamic thrust bearing performance on the basis of thermoelastohydrodynamic calculations and operational data[J]. *Proc. IMechE. Part J: J Engineering Tribology*, 2004, 218: 413–421.

[27] CLAVATSKIH S B, FILLON M. THED analysis of thrust bearings with PTFE-faced pads[J]. *ASME J. Tribol.*, 2006, 128: 49–58.

[28] MA Zhenyue, DONG Yuxin. Thermoelastiohydrodynamic lubrication of PTFE[J]. *Journal of Dalian University of Technology*, 2000, 40(12): 90–94.

[29] ZHAO Hongmei, DONG Yuxin, MA Zhenyue. The lubrication calculation of thrust bearings with pivoted supports for hydrogenerator[J]. *Large Electric Machine and Hydraulic Turbine*, 1994, 1: 8–12.

[30] AHMED S, FILLON M. Influence des deformantionsmecaniguessur les performances des buteeshydrodynamiques a geometrisfixe[C]// *Proceedings of the Second Congress on Design and Modeling of Mechanical Systems*, Monastir, Tunisia, 2007: 1–8.

[31] JIANG X, WANG J, FANG J. Thermal elastohydrodynamic lubrication analysis of tilting pad thrust bearings[J]. *Proceedings of the Institution of Mechanical Engineers, Part J: Journal of Engineering Tribology*, 2011, 225(2): 51–57.

[32] BORRÀS F X, ALMQVIST A, UKOSAARI J. *Multiphysics modeling of spring-supported thrust bearings for hydropower applications*[M]. LTU Publications, 2012.

[33] KARADERE G. The effects of the total bearing deformation on the performance of hydrodynamic thrust bearings[J]. *Industrial Lubrication and Tribology*, 2010, 62(4): 207–213.

[34] WU Zhongde, WU Junling. Design and thermo-elastic-hydrodynamic performance analysis of bi-directional thrust bearing[J]. *Large Electric Machine and Hydraulic Turbine*, 2010, 6: 26–32. (in Chinese)

[35] WU Zhongde, ZHANG Hong. Performance analysis of thrust bearing for three-gorges generator[J]. *Large Electric Machine and Hydraulic Turbine*, 2011, 2: 1–4. (in Chinese)

[36] HUANG Bin, WU Junling, WU Zhongde. Effects of support structure on lubricating properties of bi-directional thrust bearings[J]. *Journal of Drainage and Irrigation Machinery Engineering*, 2012, 30(6): 690–694.

[37] JIANG Xiulong. *TEHD analysis of tilting pad thrust bearing*[D]. Hangzhou: Zhejiang University, 2011. (in Chinese)

[38] ZHANG Lu. *Lubrication performance of thrust bearings for hydrogenerators*[D]. Tianjin: Tianjin University, China, 2008. (in Chinese)

[39] GUO Jie. Analysis of high-speed pump thrust sliding bearing's load capacity[D]. Nanjing: Nanjing Forestry University, 2012. (in Chinese)

[40] LIU Run. *Study on multi-field coupling dynamics of centrifugal compressor thrust bearing*[D]. Beijing: Beijing University of Chemical Technology, 2013. (in Chinese)

[41] YAN Qiongqiong. *Lubrication performances of thrust bearings with PTFE-faced Pads in hydro-generators*[D]. Changchun: *Jilin University*, 2014. (in Chinese)

[42] HUANG Bin, WU Zhongde. Numerical and experimental research of bidirectional thrust bearings used in pump-turbines[J]. *Proceedings of the Institution of Mechanical Engineers, Part J: Journal of Engineering Tribology*, 2012, 226(9): 795–806.

Biographical notes

ZHAI Liming, born in 1987, is currently a PhD candidate at *State Key Laboratory of Hydroscience and Engineering & Department of Thermal Engineering, Tsinghua University, China.* His research interests include bearing lubrication and rotor dynamics.
Tel: +86-10-62791262; E-mail: dlm10@mails.tsinghua.edu.cn

LUO Yongyao, born in 1980, is currently a PhD and a teacher at *State Key Laboratory of Hydroscience and Engineering & Department of Thermal Engineering, Tsinghua University, China.* His research interests include hydro turbine optimization and dynamic analysis for the fluid machinery.
E-mail: luoyy@tsinghua.edu.cn

WANG Zhengwei, born in 1962, is currently a professor and a PhD candidate supervisor at *State Key Laboratory of Hydroscience and Engineering & Department of Thermal Engineering, Tsinghua University, China.* His main research

interests include hydro turbine runner design optimization, ocean engineering, rotor dynamics.
E-mail: wzw@tsinghua.edu.cn

LIU Xin, born in 1987, is currently a PhD candidate at *State Key Laboratory of Hydroscience and Engineering & Department of Thermal Engineering, Tsinghua University, China.* His research interests include failure analysis and life prediction for the hydro turbine.
E-mail: x-liu06@mails.tsinghua.edu.cn